Silva Gabreta	vol. 29	p. 1–16	Vimperk, 2023

Morphology of glacial accumulation landforms in two Bohemian Forest cirques

Václav Duffek[1,2*], Klára Vočadlová[2] & Pavel Mentlík[2]

[1] *Faculty of Science, University of Ostrava, 30. dubna 22, CZ-70103 Ostrava, Czech Republic*
[2] *Faculty of Education, University of West Bohemia, Veleslavínova 42, CZ-30614 Plzeň, Czech Republic*
[*] duffekv@fpe.zcu.cz

Abstract
Morphological phases of moraines from north-oriented valleys are known in the Bohemian Forest. Detailed data from south-oriented valleys are still missing. This paper presents morphological phases of moraines from two valleys. Glacial landforms were defined by an accurate digital elevation model (DEM) and verified by field mapping. The extent and internal structure of the selected glacial landforms were refined by geophysical profiling. We have described 8 morphological phases of moraines in the Großer Schwarzbach cirque locality (south orientation) and 4 morphological phases of moraines in the Kleiner Rachelbach cirque locality (north orientation). In the north-oriented valley, the number of morphological phases of moraines corresponds to other north-oriented sites in the Bohemian Forest. In the south-oriented valley, the number of morphological phases of moraines exceeds the number of morphological phases of moraines in the north-oriented sites in the Bohemian Forest.

Key words: Bohemian Forest, glaciation, geomorphological mapping, electrical resistivity tomography

Introduction

The Bohemian Forest laid between mountain glaciations linked to the Alps and continental glaciations centred on the Scandinavian Peninsula in Pleistocene (Huijzer & Vandenberghe 1998, Ehlers et al. 2011). Localities in the Bohemian Massif are therefore a link in correlating palaeoenvironmental changes (Reuther 2007, Mentlík et al. 2010, Vočadlová et al. 2015). There are 8 cirques with lakes (Rathsburg 1927, Ergenzinger 1967, Steffanová & Mentlík 2007, Vočadlová 2011, Hauner et al. 2019) and several glacial cirques without lakes (Hauner 1980, Pfaffl 1997, Křížek et al. 2012, Vondrák et al. 2019) in the Bohemian Forest. Palaeoenvironmental changes have been described in detail at some sites (Bucher 1999, Raab & Völkel 2003, Reuther 2007, Mentlík et al. 2010, Vočadlová et al. 2015), but exclusively in north-facing valleys. For valleys with warm (south) orientation, older chronologies (Hauner 1980, Pfaffl 1997), or chronologies based on a digital elevation model (Hauner et al. 2019) are available.

The proxy data for paleoclimatic reconstructions can be obtained by geomorphological mapping, geomorphological analysis and subsequent dating of geomorphological landforms, particularly moraines (Mentlík et al. 2010, Chandler et al. 2018). The extent of the moraines (in addition to classical sedimentological methods) is currently being verified by non-invasive geophysical methods (MENTLÍK et al. 2010, VOČADLOVÁ 2011). One commonly used geophysical method is electrical resistivity tomography (ERT), which measures the electrical properties of the subsurface environment (LOKE 2000, HAUCK & KNEISEL 2006, KNEISEL 2006, RIBOLINI et al. 2010, TÁBOŘÍK et al. 2017).

The present regional study aims to: i) define glacial landforms in two formerly glaciated localities using an accurate DEM and field mapping, ii) refine the delineation of glacial landforms using geophysical profiling and iii) compare formerly glaciated localities with different orientation. The results will serve as a basis for deglaciation chronologies and their correlation with other chronologies of deglaciation in Central Europe.

Regional setting

The Großer Schwarzbach cirque locality (Fig. 1A) and the Kleiner Rachelbach cirque locality (Fig. 1B) were chosen for the study (names after HAUNER et al. 2019). Glacial evolution is assumed for both sites (ERGENZINGER 1967, HAUNER 1980, STEFFANOVÁ & MENTLÍK 2007, KŘÍŽEK et al. 2012, HAUNER et al. 2019, KRAUSE & MARGOLD 2019). A major difference between the sites is their orientation. The Großer Schwarzbach cirque is oriented almost to the south, whereas the Kleiner Rachelbach cirque is oriented almost to the north

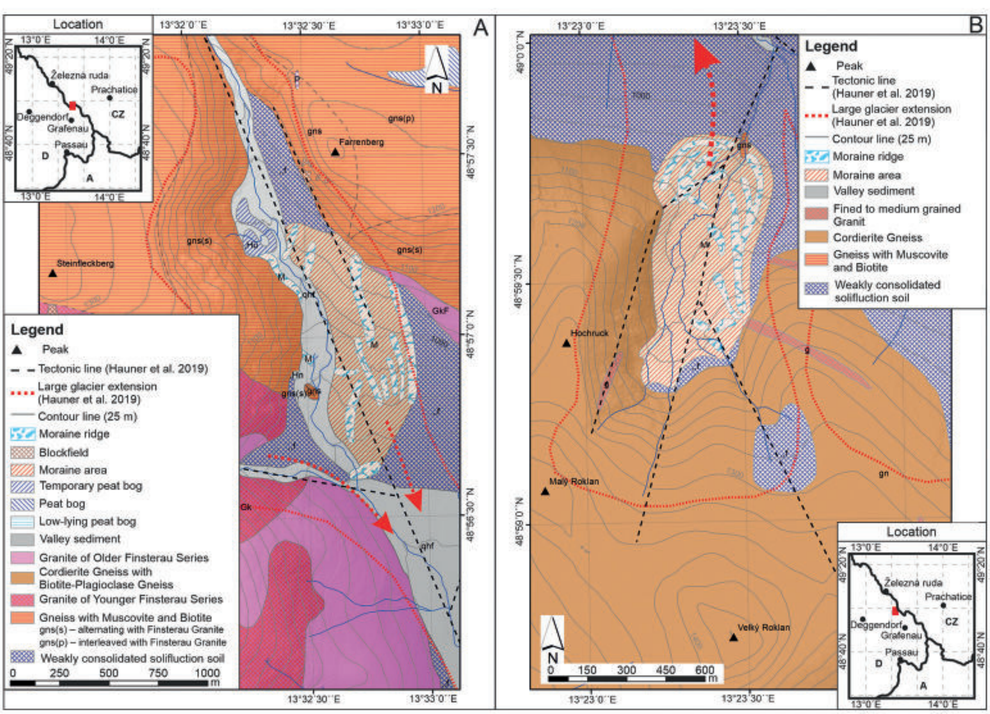

Fig. 1. Geological maps of the study localities A) the Großer Schwarzbach cirque locality; B) the Kleiner Rachelbach cirque locality) with their location in the region. Background data BAUBERGER 1977. The maps are supplemented by areas (red dotted line) of the hypothetical maximum glacier extent according to HAUNER et al. (2019) with their indicated movement (red dotted arrows).

(KŘÍŽEK et al. 2012). Therefore, the differences in the action of glacial processes (BENN & EVANS 2010, BIERMAN & MONTGOMERY 2014) and thus differences in the nature of the glaciations (BENN & EVANS 2010, BIERMAN & MONTGOMERY 2014) can be assumed. More extensive glaciation delineated by the red dotted line in Figs. 1A) and 1B) is considered at both sites (HAUNER et al. 2019, KRAUSE & MARGOLD 2019). Obviously, the bounding landforms of this glaciation would have to have been formed by a completely different, older and significantly more extensive glacial system than the glacial landforms studied at both sites. Their research is not the focus of this article.

Großer Schwarzbach cirque locality

The site is located less than 4 km northwest of the German town of Finsterau. The cirque is without a lake, but there are wetlands on the cirque floor. PFAFFL (1997) carried out geomorphological research at the site. However, this research was not based on a detailed DEM (PFAFFL 1997). HAUNER et al. (2019) provide a relative chronology of deglaciation based on a detailed DEM analysis combined with fieldwork. HAUNER (1980), PFAFFL (1997), HAUNER et al. (2019), VONDRÁK et al. (2019) suggest that there is an infilled lake of unknown depth. DUFFEK & MENTLÍK (2022) tend to favour this hypothesis based on a basic geophysical survey. The maximum elevation of the cirque wall is 1272 m a.s.l. and the minimum elevation of the cirque floor is 1016 m a.s.l. The cirque is excavated into the eastern slope of the Steinfleckberg peak (1341 m a.s.l.), but the valley is oriented almost to the south. The cirque is transected by tectonic lines with a NNW-SSE direction (HAUNER et al. 2019). According to BAUBERGER (1977), the locality is composed of gneiss alternating with granite (see Fig. 1A).

Kleiner Rachelbach cirque locality

The Kleiner Rachelbach cirque is located less than 12 km southeast of the town of Zwiesel. There are only wetlands and peatlands on the cirque floor (HAUNER et al. 2019). HAUNER et al. (2019) provide a relative chronology of deglaciation based on DEM analysis combined with fieldwork. The presence of infilled lake sediments of unknown depth is assumed (HAUNER 1980, HAUNER et al. 2019, VONDRÁK et al. 2019). The maximum elevation of the cirque wall is 1281 m a.s.l. and the minimum elevation of the cirque floor is 1070 m a.s.l. (KŘÍŽEK et al. 2012, HAUNER et al. 2019). The cirque is excavated into the northern slopes of the Kleiner Rachel (1399 m a.s.l.) and Großer Rachel (1453 m a.s.l.) peaks. The main tectonic lines run SSW-NNE (HAUNER et al. 2019). According to BAUBERGER (1977), the locality is composed of gneiss with granite veins (see Fig. 1B).

METHODOLOGY

A 4 step methodology was designed to establish the morphology of both sites (Fig. 2). The basis was a detailed LIDAR (DEM) which was loaned by the Bavarian Forest National Park Authority. We used DGM 1 m (LDBV 2022) with high resolution (1×1 meter). Height accuracy is in centimetres and mean error in height is +/– 0.5 m (LDBV 2022).

In the first step, landforms were defined on the basis of the DEM and its derivatives (hillshaded relief, slope gradient and slope orientation) according to MINÁR & EVANS (2008).

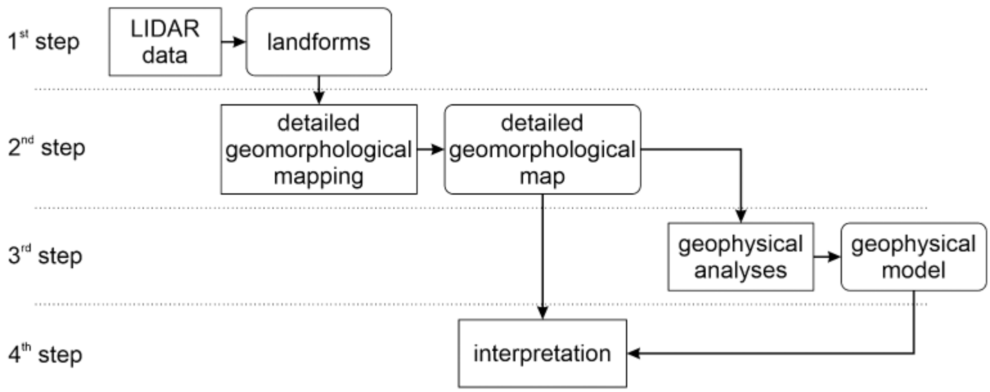

Fig. 2. Research methodology.

In the second step, the landforms were verified in the field by geomorphological mapping (according to SMITH et al. 2011, OTTO & SMITH 2013, CHANDLER et al. 2018) and their boundaries were further refined. The landforms were plotted into a geographical information system (GIS). Finally, the necessary analyses and determination of the assumed genesis of the landforms were carried out based on the GIS. In the third step, a geophysical survey of potentially glacial landforms was carried out (according to the methodology below) in order to analyse subsurface manifestations of particular landforms. The fourth step involved the interpretation of the geomorphological map and the geophysical models. This step involved a synthesis of the geomorphological and geophysical interpretations, which we use as a means of adding knowledge to the understanding of the origin and evolution of the different landforms.

The selected landforms were analysed using electrical resistivity tomography (LOKE 2000, SCHROTT & SASS 2008, TÁBOŘÍK et al. 2017). The ARES II (Automatic Resistivity System II) was used for profiling. All measurements were made in a Schlumberger electrode arrangement, because both vertical and horizontal subsurface manifestations were assumed at the sites (LOKE 2000, SCHROTT & SASS 2008). The electrode spacing was 5 m for all profiles. Additional characteristics of the profiles are given in Table 1 and the detailed location of the profiles is shown in Fig. 3A and 4A. The measured data were processed in Res2Dinv (GEOTOMO SOFTWARE, 2018) using tomographic inversion and topographic corrections (sensu LOKE 2000). The topography was derived in ArcMap (ESRI, 2021) from the DEM. Depending on the assumed internal structures (LOKE et al. 2015), least square inversion or robust inversion was used (see Table 1). To ensure the lowest RMS (root mean square)/ABS (absolute) error, the damping factor values were optimized for each resistivity model (e.g. SASAKI 1992, LOKE et al. 2015).

Table 1. Additional characteristics of geophysical profiles.

ERT profile	Length (m)	Direction	Type of inversion	RMS/ABS error
Gr. Schwarzbach B	395	SSE–NNW	robust	3.8
Gr. Schwarzbach C	315	W–E	least-squares	5.3
Kl. Rachelbach B	235	WNW–ESE	least-squares	5.6
Kl. Rachelbach C	515	E–W	least-squares	7.6

Results

Großer Schwarzbach

Several significant (with an elevation of over 3 metres above the surrounding relief) and non-significant (with an elevation of less than 3 metres above the surrounding relief or with only a stepped character) moraine ridges were identified at the Großer Schwarzbach site. Table 2 lists the detailed morphometric characteristics of the moraine ridges, and their locations are mapped in Fig. 3. The last moraine is an accumulation directly adjacent to the assumed cirque floor (14 in Fig. 3). The extensive (80 000 m^2) and almost flat bottom of the cirque is connected to a relatively steep cirque wall (slope of over 80°) with many rock steps.

The geophysical model B (Fig. 3B) at the Großer Schwarzbach locality can be divided into six parts (1–6 in Fig. 3B) based on the subsurface resistivity distribution. The first part (1 in Fig. 3B) is characterized by a body with extremely high resistivities. The second part (2 in Fig. 3B) consists of a fairly pronounced horizontal transition from high resistivities to low resistivities (indicated by the black dotted line). The third section (3 in Fig. 3B) is characterized by a compact body with minimal resistivity that extends to a depth of about 30 metres. The fourth section (4 in Fig. 3B) is composed of a near-surface layer of intermediate resistivities that overlies a low-resistivity zone at a depth of 5–10 metres. The fifth part (5 in Fig. 3B) is characterised by a very shallow near-surface low-resistivity layer that overlies the medium-resistivity layer. Between the fourth and fifth parts, a gradual horizontal transition (indicated by the black dashed line) from low resistivity to medium resistivity can be observed at a depth of 15–25 m. In the sixth section (6 in Fig. 3B), the layer of medium resistivities rises to the surface.

The parts of the model correspond to the landforms identified by geomorphological mapping (Fig. 3A). The first part of the model (1 in Fig. 3B) corresponds to the assumed moraine ridge 14 that encloses the cirque floor (14 in Fig. 3A). The second to fifth parts of the model (2–5 in Fig. 3B) correspond to the cirque floor (Fig. 3) and the sixth part of the model (6 in Fig. 3B) corresponds to the cirque wall foot (Fig. 3). The glacial sediments of the assumed frontal moraine ridge show extremely high resistivities in the model (Fig. 3B). In contrast, the cirque floor (at least in its southern part) is manifested by extremely low resistivities (Fig. 3B), reaching depths of up to 30 m.

Geophysical model C (Fig. 3C) at the Großer Schwarzbach locality is strongly heterogenous. Based on the subsurface resistivity distribution, it can be divided into a number of parts (14 in total). In the model, parts can be observed that: i) are characterized by a shallow

Table 2. Morphometric characteristics of moraine ridges in the Großer Schwarzbach locality.

Morphometric characteristics of moraine ridges		
No.	**Elevation**	**Notes**
1	12 m	Followed by a degraded, less significant step-like moraine.
2	4 m	Sequence of 5 relatively narrow and strongly elongated moraines.
3	7 m	Sequence of 5 relatively narrow and strongly elongated moraines. Large granite blocks on the surface.
4	4 m	Sequence of 5 relatively narrow and strongly elongated moraines.
5	6 m	Sequence of 5 relatively narrow and strongly elongated moraines. Large granite blocks on the surface.
6	8 m	Sequence of 5 relatively narrow and strongly elongated moraines.
7	6 m	–
8	3 m	–
9	up to 3 m	Peatlands behind the ridge higher up the slope.
10	up to 3 m	Peatlands behind the ridge higher up the slope.
11	up to 3 m	Peatlands behind the ridge higher up the slope.
12	4 m	Degrades higher up the slope (elevation decreases to less than 2 metres).
13	4 m	Degrades higher up the slope (elevation decreases to a step-like moraine).
14	5 m	Encloses wetlands and peat bogs in the cirque floor. Large granite blocks on the surface.

near-surface layer of medium resistivities that sits on a layer of high to extremely high resistivities (parts 2, 4, 7, 9, 11, 13 in Fig. 3C); ii) are characterized by protruding high resistivities to the surface (parts 1, 3, 6, 8, 10, 12, 14 in Fig. 3C). In the fifth part of the model (5 in Fig. 3C), the near-surface zone of medium resistivities manifests itself to greater depths (up to 15 m), where it again sits on the zone of higher resistivities. The high resistivity zone, which can be observed across the entire profile (indicated by the black dotted line), gradually transits to low resistivity at depth. The depth of this transition varies along the profile. It is approximately 35 metres at the beginning of the profile and approximately 15 metres at the end of the profile (Fig. 3C).

The subsurface distribution of resistivity partly corresponds to the results of the geomorphological mapping (Fig. 3). The first and second parts of the model (1, 2 in Fig. 3C) correspond to the valley floor. The third part forms a kind of transition. The fourth and fifth parts (4, 5 in Fig. 3C) correspond to moraine 6. Moraine 5 corresponds to the sixth part and part of the seventh part of the model (6, 7 in Fig. 3C). The rest of the seventh part of the model (7 in Fig. 3C) is almost identical to moraine 4. The positions of the eighth and ninth parts of the model (8, 9 in Fig. 3C) are almost identical to moraine 3, and moraine 2 agrees with the position of the twelfth and thirteenth parts of the model (12, 13 in Fig. 3C). Due to the presence of a high-resistivity layer across the entire profile (indicated by the black dotted line), each

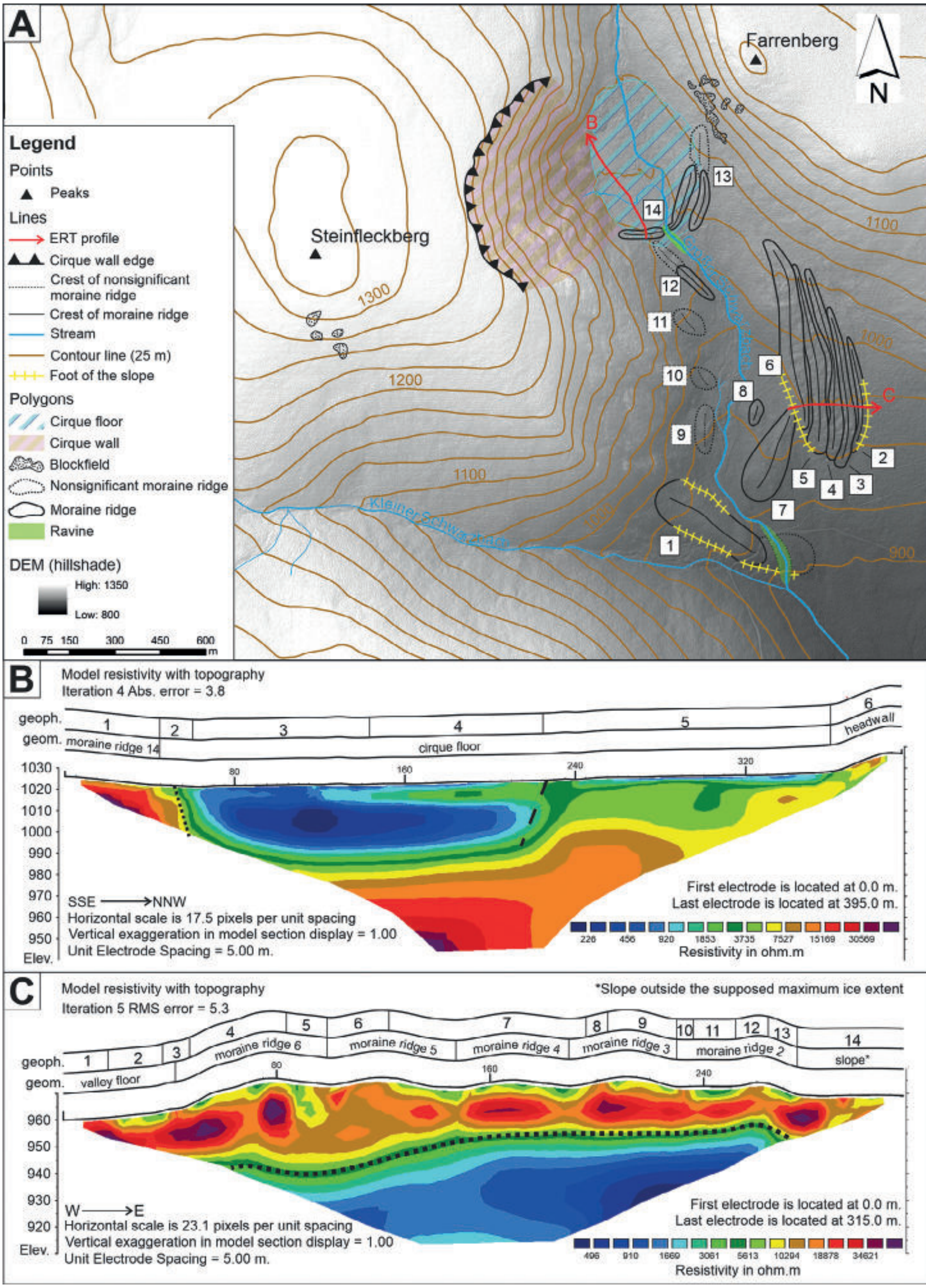

Fig. 3. Results of research in the Großer Schwarzbach cirque locality. A) Map showing selected landforms (the underlying data was loaned by the Bavarian Forest National Park Authority). B) and C) ERT subsurface resistivity distribution models with mapped landforms (description corresponds to Fig. 3A). The black dotted and dashed lines in model B indicate the probable subsurface horizontal interfaces. The black dotted line in model C approx. defines the high-resistivity layer.

moraine is characterized by high resistivities. In addition, we observe a local increase in resistivity at moraines 2–6 (in Fig. 3C). An increase in resistivity can also be observed at the beginning of the profile to where the end of moraine 7 (7 in Fig. 3) extends.

Kleiner Rachelbach

Relatively few moraines have been identified at the Kleiner Rachelbach cirque site (cf. Fig. 3A and Fig. 4A). Table 3 lists the detailed morphometric characteristics of the moraine ridges. Their locations are mapped in Fig. 4.

The entire site is enclosed by a hummocky relief to the north (Fig. 4A). No compact and coherent moraine ridge could be identified in the field in this hummocky relief. This undulating relief is limited in the north by a steep slope (gradient of over 60°), which transits into a slope with a gradient of about 20° at an altitude between 1025 and 1000 m a.s.l. The area of undulating relief is dissected by the Kleiner Rachelbach Stream and its tributaries, which form gullies (Fig. 4A). The cirque has a stepped structure. The east-facing slopes of the cirque wall, with a high occurrence of rock steps and tors drop steeply to the bottom, where they produce a marked change in slope (from an average of 8° at the floor to an average of 35° and a maximum of 80° in the cirque wall). Moraine ridge 6 (Fig. 4) creates a depression (with an area of 6 266 m^2) between the original slope and the moraine ridge. The depression is clearly visible in the field (Fig. 4D).

The geophysical model B in the Kleiner Rachelbach locality (Fig. 4B) can be divided into three parts based on the subsurface resistivity distribution. In the first part (1 in Fig. 4B), we can observe a roughly 5 m thick near-surface layer of intermediate resistivities superimposing a compact body with extremely high resistivities. This body is over 20 metres thick. The second part of the model (2 in Fig. 4B) is characterized by an extremely low resistivity body at the surface, which manifests down to a depth of 10 metres. The thickness of this low-resistivity body decreases towards the east. The third part of the model (3 in Fig. 4B) consists of a near-surface layer of medium resistivities that overlies a layer of higher resistivities.

The division of the model into three parts (Fig. 4B) closely corresponds to the landforms identified by the geomorphological mapping. The first part of the model (1 in Fig. 4B) corresponds to the slope with the presumed glacial sediment (Fig. 4A), but also to the mapped ridge of the presumed lateral moraine 6. The second part of the model (2 in Fig. 4B) clearly agrees with the depression between moraine 6 (6 in Fig. 4) and the higher slope. The third part of the model (3 in Fig. 4B) corresponds to a slope outside the supposed maximum ice extent (Fig. 4). The hypothetical extension of the higher slope course (black dotted line in Fig. 4B) implies the deposition of the moraine ridge 6 mass on the original slope.

Geophysical model C in the Kleiner Rachelbach locality (Fig. 4C) can be divided into 11 parts based on the subsurface resistivity distribution. A high-resistivity layer can be observed across the entire model (bounded by the white dashed line in Fig. 4C). We can assume a continuation of this layer further east (marked by the black dotted line with the question mark in Fig. 4C) at the end of the profile. The high-resistivity layer is significantly interrupted by a low-resistivity body in part 6 (6 in Fig. 4C). In some parts of the model (2, 4, 8 in Fig. 4C), a shallow near-surface layer of intermediate resistivities overlies the high-resistivity layer. In some parts of the model (1, 3, 5, 7, 9, 11 in Fig. 4C), the high

Table 3. Morphometric characteristics of moraine ridges in the Kleiner Rachelbach locality.

Morphometric characteristics of moraine ridges		
No.	**Elevation**	**Notes**
1	over 10 m	Clearly visible in the field.
2	4 m	–
3	3 m	Encloses lower step of the cirque floor. Relatively narrow and strongly elongated.
4	up to 1 m	Encloses lower step of the cirque floor.
5	up to 3 m	Relatively narrow and strongly elongated.
6	3 m	Is undercut by stream on the south.
7	up to 2 m	Encloses higher step of the cirque floor.

resistivities protrude directly to the surface. In part 10 of the model (10 in Fig. 4C), the absolute values of the resistivities in the high-resistivity layer are slightly reduced. However, there are still relatively high resistivities. The thickness of the high-resistivity layer (bounded by the white dashed line) decreases along the profile (from about 25 m at the beginning of the profile to about 15 m at the end of the profile). The subsurface at greater depths is characterised by much lower resistivities with the presence of several extremely low resistivity bodies.

The subsurface resistivity distribution (Fig. 4C) partially corresponds to the results of the geomorphological mapping (Fig. 4). The first five parts in the model (1–5 in Fig. 4C) correspond to the assumed lateral moraine 1. The distinct interruption of the high-resistivity zone by a low-resistivity body in the sixth part of the model (6 in Fig. 4C) corresponds to the stream and its near surroundings (Fig. 4). Parts 7, 8, 9 and some of part 10 (7, 8, 9, 10 in Fig. 4C) correspond to the mapped hummocky terrain (Fig. 4), which is manifested by a number of depressions and elevations on the surface. The second stream is not significant on the model (Fig. 4C). The assumed lateral moraine 2 (2 in Fig. 4A) at the end of the profile is also not significantly delineated on the geophysical model (Fig. 4C). The slope with no assumed glacial alteration shows a local increase in resistivity on the model and corresponds to part 11 in Fig. 4C.

Morphological phases of moraines

The morphological phases of moraines for both sites is shown in Fig. 5. 8 morphological phases of moraines can be recognised (Sch1–Sch8 in Fig. 5A) in the Großer Schwarzbach locality (Fig. 5A). The second, third and fourth phases (Sch2–Sch4 in Fig. 5A) are defined by only one moraine. The other phases are defined by two or more moraines. 4 morphological phases of moraines can be identified (Ro1–Ro4 in Fig. 5B) in the Kleiner Rachelbach locality (Fig. 5B), but the last two phases are each defined by only one non-significant moraine (moraines 5 and 7 in Fig. 4A).

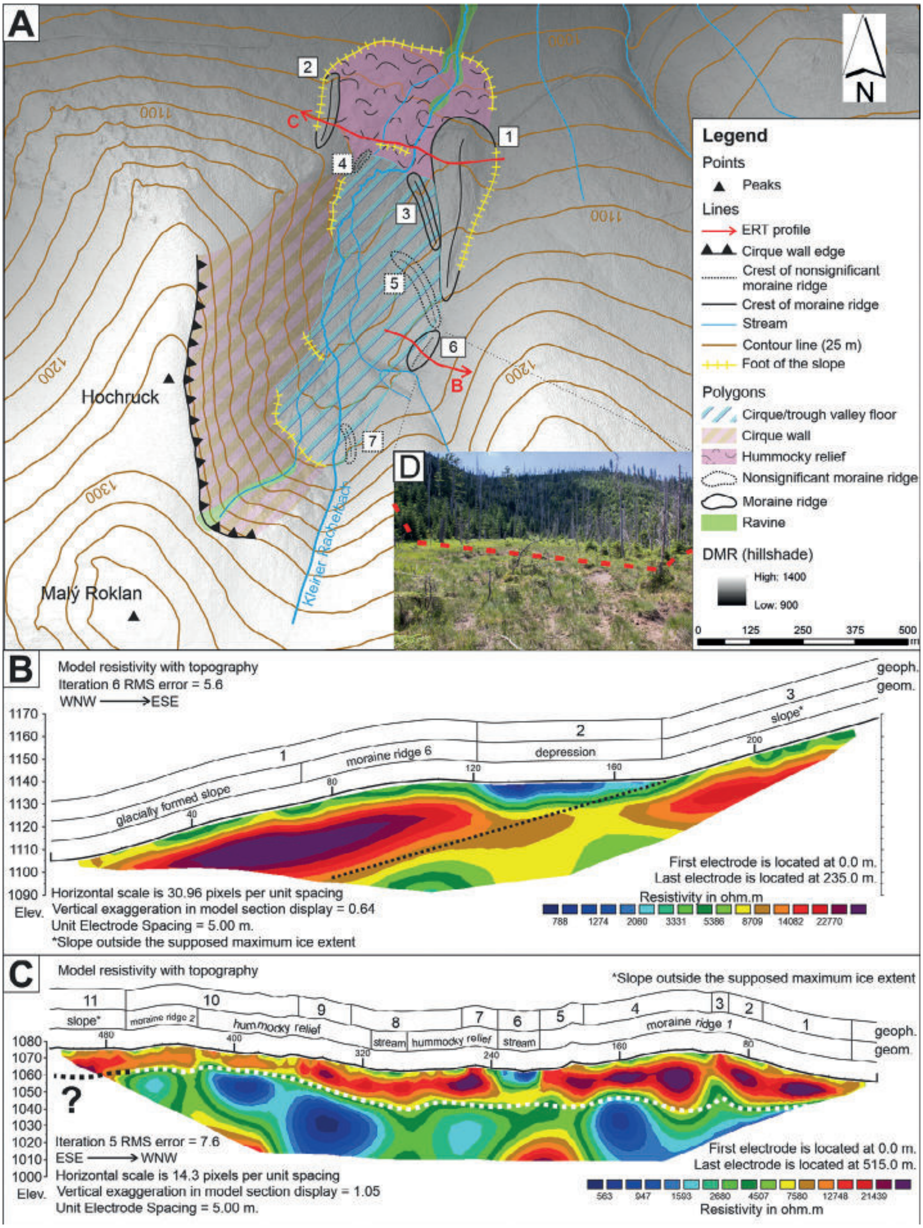

Fig. 4. Results of research in the Kleiner Rachelbach cirque locality. A) Map showing selected landforms (the underlying data was loaned by the Bavarian Forest National Park Authority). B) and C) ERT subsurface resistivity distribution models with mapped landforms (description corresponds to Fig. 4A). The black dotted line in model B marks the hypothetical course of the original slope. The white dotted line in model C defines the high-resistivity layer and the black dotted line defines the assumed continuation of the high-resistivity layer further to the WNW. Stream corresponds to the stream and near surroundings. D) Depression between assumed moraine ridge 6 and the higher slope. The red dashed line marks the surface of the relief.

Discussion

Geophysical-geomorphological interpretation

All moraines analysed by electrical resistivity tomography appear as extremely high-resistivity bodies in the resulting models (Fig. 3 and 4). Extremely high resistivities in mountainous environments can be manifestations of permafrost, rock glacier ice, a blockfield or blockstream, debris flow, and other slope process accumulations or glacial sediments (Loke 2000, Musset & Khan 2000, Hauck & Kneisel 2006, Sass 2006, Schrott & Sass 2008, Ribolini et al. 2010). The current occurrence of permafrost or active rock glaciers is not expected in the Bohemian Forest (Nývlt et al. 2011, Hauner et al. 2019). The morphology of the moraines does not correspond to the manifestations of a blockfield or a blockstream (sensu Steijn et al. 2002, Rea 2007). There are no tors above the accumulations. At both sites, no scarps were found in the vicinity of the investigated moraines, indicating a mass-wasting origin of the accumulations (Geertsema & Chiarle 2013, Bierman & Montgomery 2014, Hungr et al. 2014). The narrow and elongated forms of the accumulations (especially at moraines 2, 3, 4, 5, 6 in the Großer Schwarzbach locality and at moraines 1 and 3 in the Kleiner Rachelbach locality) also do not support the hypothesis

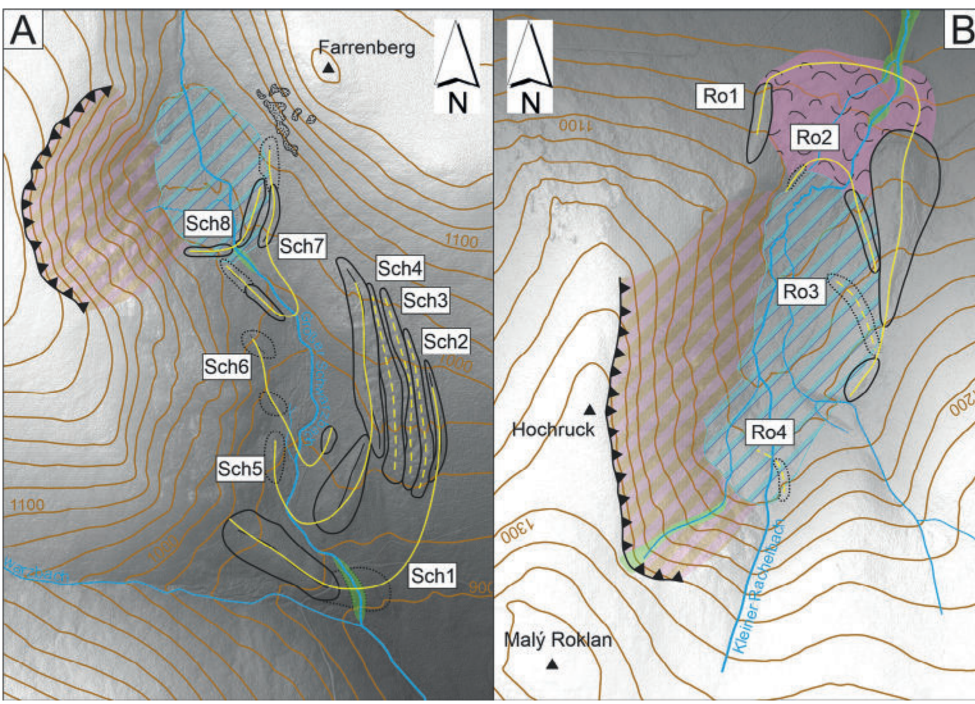

Fig. 5. Morphological phases of moraines in both localities (A) Großer Schwarzbach, B) Kleiner Rachelbach). Yellow lines represent supposed extension of glaciers during a particular phase based on the moraine ridges. Note yellow dashed lines in Großer Schwarzbach and Kleiner Rachelbach represent phases which are defined by only one moraine ridge.

of a mass-wasting origin (BIERMAN & MONTGOMERY 2014, HUNGR et al. 2014). These facts only support the glacial genesis of the analysed ridges.

The accumulation landform of 5 moraine ridges at the Großer Schwarzbach site (Fig. 3) provides very atypical evidence of glaciation development for the Bohemian Forest. All the moraines show increased resistivity. Moraines 6 and 5 (6, 5 in Fig. 3) appear significantly thicker than the other moraines (4, 3, 2) on the resistivity model (Fig. 3C). This could indicate the different ages of the moraines (HUBBARD & GLASSER 2005, BENN & EVANS 2010).

High resistivities at the end of geophysical profile C in Kleiner Rachelbach locality (Fig. 4C) could correspond to glacial sediments (LOKE 2000, MENTLÍK et al. 2010, RIBOLINI et al. 2010, TÁBOŘÍK et al. 2017). However, according to geomorphological analysis, this part does not appear to be glacially altered. It is thus possible to consider a more extensive glaciation, which is assumed by HAUNER et al. (2019) or KRAUSE & MARGOLD (2019). Another alternative is the possible presence of an older buried glacial landform, as described by DUFFEK & MENTLÍK (2022) near the Prášilské Lake, or a landform of unknown origin.

The very low resistivities in the B models in both localities (Fig. 3B and 4B) most likely indicate historical depressions (similar to MENTLÍK et al. 2010, VOČADLOVÁ et al. 2015, VONDRÁK et al. 2021) that are now (according to resistivity characteristics) filled with moistened sediments (LOKE 2000, MENTLÍK et al 2010). In the Großer Schwarzbach cirque locality (Fig. 3), low resistivities support the hypothesis of an infilled cirque lake, which is also mentioned by other authors (PFAFFL 1997, KŘÍŽEK 2012, HAUNER et al. 2019, DUFFEK & MENTLÍK 2022). In the Kleiner Rachelbach locality (Fig. 4), it is most likely an infilled depression between the moraine and the adjacent slope (similar to VOČADLOVÁ et al. 2015). The sedimentary records from both sites could thus be interesting paleoclimatic proxies (MENTLÍK et al. 2010, VOČADLOVÁ et al. 2015, VONDRÁK et al. 2021).

Correlation of the morphological phases of moraines

The established morphological phases of moraines in the Kleiner Rachelbach cirque locality is partly consistent with other morphological phases of moraines in the region (Table 4), which are also based on detailed geomorphological mapping (REUTHER et al. 2011, MENTLÍK et al. 2013, VOČADLOVÁ et al. 2015). Based on a DEM, HAUNER et al. (2019) propose the existence of 2 LGM moraines (LGM double wall) and 4 deglaciation moraines at this site, similar to the Kleiner Arber Lake locality (REUTHER et al. 2011). However, they define the first four phases (LGM double wall and two regressive moraines) in the hummocky moraine relief locality (HAUNER et al. 2019), where no continuous moraines have been mapped in the field.

The morphological phases of moraines in the Großer Schwarzbach cirque locality is not consistent with other morphological phases of moraines in the region (Table 4), which are also based on detailed geomorphological mapping (REUTHER et al. 2011, MENTLÍK et al. 2013, VOČADLOVÁ et al. 2015). HAUNER et al. (2019) define the 2 LGM moraines (LGM double wall) and 5 deglaciation moraines in this locality using a DEM. The number of morphological phases of moraines in the Großer Schwarzbach cirque locality is approximately twice the number of morphological phases of moraines in the Kleiner Rachelbach cirque locality, Laka lake, Prášilské Lake, Černé Lake and Kleiner Arber Lake (REUTHER et al. 2011, MENTLÍK et al. 2013, VOČADLOVÁ et al. 2015). This difference could be due to the spatial

Table 4. Morphological phases of moraines in the Großer Schwarzbach and Kleiner Rachelbach sites compared to other local morphological phases of moraines in the region.

Locality	Großer Schwarzbach[a]	Kleiner Rachelbach[a]	Laka Lake[b]	Prášilské Lake[b]	Černé Lake[c]	Kleiner Arber Lake[d]
Relative chronology	Sch1	Ro1	Laka 1	Pras 1	M1	WIa
	Sch2	Ro2	Laka 2	Pras 2	M2	WIb
	Sch3	Ro3		Pras 3	M3	WII
	Sch4	Ro4			M4	WIV
	Sch5				M5	
	Sch6					
	Sch7					
	Sch8					
Aspect	SSE	NNE	NNE	NNE	NE	N
Volume (106 m^3)	62.04	78.84	96.70	11.02*	173.74	353.75

Volume based on KŘÍŽEK et al. 2012. *only lower cirque (based on MENTLÍK et al. 2010). [a] this study, [b] MENTLÍK et al. 2013, [c] VOČADLOVÁ et al. 2015, [d] REUTHER 2007.

(south) orientation of the site and the associated higher glacier activity (BENN & EVANS 2010, BIERMAN & MONTGOMERY 2014).

There are other cirques oriented to the south in the Bohemian Forest (KŘÍŽEK et al. 2012). For example, Südlicher Rachel cirque locality (according to HAUNER et al. 2019), where HAUNER et al. (2019) defined the 2 LGM moraines (LGM double wall) and 5 deglaciation moraines. This supports the hypothesis of higher glacier activity in south-facing localities of the Bohemian Forest.

CONCLUSION

The morphological phases of moraines were created on the basis of the position of moraine ridges that were defined using the detailed DEM and verified by field geomorphological mapping. A glacial origin was proved for selected accumulation landforms based on the analysis of the subsurface environment (by ERT) and morphometry of the moraines. In addition, the geophysical analysis supports the hypothesis of an infilled lake in the Großer Schwarzbach cirque locality and reveals an infilled depression in the Kleiner Rachelbach cirque locality. The research identified 8 morphological phases of moraines in the Großer Schwarzbach cirque locality and 4 morphological phases of moraines in the Kleiner Rachelbach cirque locality. The conclusions outlined above will serve as the basis for further geomorphological and palaeoclimatic investigations of the sites and are the prerequisite for the application of geochronological methods.

Software. Mapping of glacial features and the DEM analyses were carried out in ArcMap 10.8.1 (ESRI 2021). Tomographic inversions were carried out in Res2Dinv (GEOTOMO SOFTWARE 2018).

Acknowledgements. This paper was supported by a grant from the Faculty of Education, University of West Bohemia (number: GRAK 2022 DS/02). The authors would like to thank the Bavarian Forest National Park Administration for the loan of the detailed digital elevation model data and for the research permission. We thank J.M. King for translation and language correction. We also thank Mr. Hauner and one anonymous reviewer for their comments which improved the manuscript.

References

Bauberger W., 1977: Nationalpark Bayerischer Wald. *Erläuterungen zur Geologischen Karte von Bayern, Blatt 7046 Spiegelau und 7047 Finsterau* [*Explanatory notes to the Geological Map of Bavaria, sheet 7046 Spiegelau and 7047 Finsterau*], München, 183 pp. (in German).

Benn D. & Evans D., 2010: *Glaciers and Glaciation*. Routledge, 816 pp.

Bierman P.R. & Montgomery D.R., 2014: *Key Concepts in Geomorphology*. W.H. Freeman and Company Publishers, 494 pp.

Bucher M., 1999: Der glaziale Formenschatz im Gebiet um den Kleinen Arbersee (Bayerischer Wald) Glacial landforms in the area of Kleiner Arbersee]. Z. *Geomorpologie N.F., Suppl.-Bd.*, 113: 45–58 (in German).

Chandler B.M.P., Lovell H., Boston C.M., Lukas S., Barr I.D., Benediktsson Í.Ö., Stroeven A.P., 2018: Glacial geomorphological mapping: A review of approaches and frameworks for best practice. *Earth-Science Reviews*, 185: 806–846.

Duffek V. & Mentlík P., 2022: Geophysical survey of glacial landscape in four Bohemian Forest cirques. *Silva Gabreta*, 28: 1–16.

Ehlers J., Gibbard P.L. & Hughes P.D. (eds), 2011: *Quaternary Glaciations – Extent and Chronology: A Closer Look*. Elsevier, 1108 pp.

Ergenzinger P., 1967: Die eiszeitliche Vergletscherung des Bayerischen Waldes [The ice age glaciation of the Bavarian Forest]. *Eiszeitalter und Gegenwart* (E&G Quaternary Science Journal), 18: 152–168. (in German).

Geertsema M. & Chiarle M., 2013: Mass-Movement Causes: Glacier Thinning. In: *Treatise on Geomorphology*, Shroder J.F., Marston R.A. & Stoffel M. (eds) *Mountain and Hillslope Geomorphology*, 7: 217–222.

Hauck C. & Kneisel C., 2006: Application of Capacitively-coupled and DC Electrical Resistivity Imaging for Mountain Permafrost Studies. *Permafrost and Periglacial Process*, 17: 169–177.

Hauner U., 1980: *Untersuchungen zur klimagesteuerten tertiären und quartären Morphogenese des Inneren Bayerischen Waldes (Rachel-Lusen) unter besonderer Berücksichtigung pleistozän kaltzeitlicher Formen und Ablagerungen* [*Investigations on the climate-controlled Tertiary and Quaternary morphogenesis of the Inner Bavarian Forest (Rachel-Lusen) with special emphasis on Pleistocene cold-age forms and deposits*]. Regensburger Geographische Schriften, 14: 198 pp. (in German).

Hauner U., Lehrberger G. & Brugger M., 2019: *Der Naturraum Bayerischer Wald – Šumava in den Eiszeiten* [*The natural region of the Bavarian Forest – Šumava in the ice ages*]. Nationalpark Bayerischer Wald, Wissenschaftliche Reihe, Heft 20,132 pp. (in German).

Hubbard B. & Glasser N., 2005: *Field Techniques in Glaciology and Glacial Geomorphology*. J. Wiley & Son, 400 pp.

Huijzer B. & Vandenberghe J., 1998: Climatic reconstruction of the Weichselian Pleniglacial in northwestern and central Europe. *Journal of Quaternary Science*, 13: 391–417.

Hungr O., Leroueil S. & Picarelli S., 2014: The Varnes classification of landslide types, an update. *Landslides*, 11: 167–194.

Kneisel C., 2006: Assessment of subsurface lithology in mountain environments using 2D resistivity imaging. *Geomorphology*, 80: 32–44.

Krause D. & Margold M., 2019: Glacial geomorphology of the Šumava / Bayerischer Wald mountains, Central Europe. *Journal of Maps*, 15: 719–725.

Křížek M., Vočadlová K. & Engel Z., 2012: Cirque overdeepening and their relationship to morphometry. *Geomorphology*, 139–140: 495–505.

LDBV, 2022: Landesamtes für Digitalisierung, Breitband und Vermessung. Digitales Geländemodell. Online https://www.ldbv.bayern.de/service/kundenservice.html (accessed on 25 June 2022).

Loke M.H., 2000: *Electrical imaging surveys for environmental and engineering studies. A practical guide to 2-D and 3-D surveys*. Geotomo software (1997–2000), 67 pp. Online http://www.geotomosoft.com (accessed on 30 April 2020).

Loke M.H., Kiflu H., Wilkinson P.B., Harro D. & Kruse S., 2015: Optimized arrays for 2D resistivity surveys with combined surface and buried arrays. *Near Surface Geophysics*, 13: 505–517.

Mentlík P., Minár J., Břízová E., Lisá L., Tábořík P. & Stacke V., 2010: Glaciation in the surroundings of Prášilské Lake (Bohemian Forest, Czech Republic). *Geomorphology*, 117: 181–194.

Mentlík P., Engel Z., Braucher R., Léanni L. & Aster Team, 2013: Chronology of the Late Weichselian glaciation in the Bohemian Forest in Central Europe. *Quaternary Science Reviews*, 65: 120–128.

Minár J. & Evans I.S., 2008: Elementary forms for land surface segmentation: the theoretical basis of terrain analysis and geomorphological mapping. *Geomorphology*, 95: 236–259.

Musset A.E. & Khan A.M., 2000: *Looking into the Earth. An Introduction to Geological Geophysics*. London. Cambridge University Press. 492 pp.

Nývlt D., Engel Z. & Tyráček J., 2011: *Pleistocene Glaciations of Czechi*a. In: *Quaternary Glaciations – Extent and Chronology A: Closer Look*, Ehlers J., Gibbard P.L. & Hughes P.D. (eds) Elsevier, 37–46.

Otto J.-C. & Smith M.J., 2013: *Geomorphological mapping*. In: *Geomorphological Techniques (Online Edition)*. Clarke L. (ed.) British Society for Geomorphology: 344–364.

Pfaffl F., 1997: Das Bärnriegel-Kar und seine Moränenlandschaft im Nationalpark Bayerischer Wald bei Finsterau [The Bärnriegel-Kar and its moraine landscape in the Bavarian Forest National Park near Finsterau]. *Der Bayerischer Wald*, 11(2): 22–23 (in German).

Raab T. & Völkel J., 2003: Late Pleistocene glaciation of the Kleiner Arbersee area in the Bavarian Forest, south Germany. *Quaternary Science Reviews*, 22: 581–593.

Rathsburg A., 1927: Die Gletscher des Böhmerwaldes zur Eiszeit [Glaciers of the Bavarian Forest in the ice age]. *Berichte der naturwissenschaftlichen Gesellschaft in Chemnitz*, 22: 65–161 (in German).

Rea B.R., 2007: *Periglacial landforms, rock forms: Blockfields (Felsenmeer)*. In: *Encyclopaedia of Quaternary Science*, Elias S.A. & Mock C.J. (eds) Elsevier: 2225–2236.

Reuther A.U., 2007: Surface exposure dating of glacial deposits from the last glacial cycle. Evidence from the Eastern Alps, the Bavarian Forest, the Southern Carpathians and the Altai Mountains. *Relief Boden Palaeoklima*, 21: 1–213.

Reuther A.U., Fiebig M., Ivy-Ochs S., Kubik P.W., Reitner J.M., Jerz H. & Heine K., 2011: Deglaciation of a large piedmont lobe glacier in comparison with a small mountain glacier – new insight from surface exposure dating. Two studies from SE Germany. *Quaternary Science Journal*, 60: 248–269.

Ribolini A., Guglielmin M., Fabre D., Bodin X., Marchisio M., Sartini S., Spagnolo M. & Choeneich P., 2010: The internal structure of rock glaciers and recently deglaciated slopes as revealed by geoelectrical tomography: insights on permafrost and recent glacial evolution in the Central and Western Alps (Italy–France). *Quaternary Science Reviews*, 29: 507–521.

Sasaki Y., 1992: Resolution of resistivity tomography inferred from numerical simulation. *Geophysical Prospect*, 40: 453–463.

Sass O., 2006: Determination of the internal structure of alpine talus using different geophysical methods (Lechtaler Alps, Austria). *Geomorphology*, 80: 45–58.

Schrott L. & Sass O., 2008: Application of field geophysics in geomorphology: advances and limitations exemplified by case studies. *Geomorphology*, 93: 55–73.

Smith M.J, Griffiths J. & Paron P. (eds), 2011: *Geomorphological Mapping: methods and applications.* Elsevier, 958 pp.

Steffanová P. & Mentlík P., 2007: Comparison of morphometric characteristics of cirques in the Bohemian Forest. *Silva Gabreta*, 13: 191–204.

Steijn Van H., Boelhouwers J., Harris S. & Hétu B., 2002: Recent research on the nature, origin and climatic relations of blocky and stratified slope deposits. *Progress in Physical Geography*, 26/4: 551–575.
Tábořík P., Gebauer J., Duras R. & Bláha P., 2017: The mystique of ERT. *Exploration Geophysics, Remote Sensing and Environment (EGRSE)*, 24/2: 28–38.
Vočadlová K., 2011: Development of Pleistocene glaciation in the Czech part of the Šumava Mts. (Case study of the Černé and Čertovo Lakes).Ms., PhD thesis, Univerzita Karlova v Praze, Praha, 221 pp. (Library of the Faculty of Sciences, Charles University).
Vočadlová K., Petr L., Žáčková P., Křížek M., Křížová L., Hutchinson S.M. & Šobr M., 2015: The Lateglacial and Holocene in Central Europe: a multi-proxy environmental record from the Bohemian Forest, Czech Republic. *Boreas*, 44: 769–784.
Vondrák D., Kopáček J., Kletetschka G., Chattová B., Suchánek V., Tátosová J. & Kuneš P., 2019: Lithostratigraphy and age of the Bohemian Forest lake sediments: A first assessment. *Geoscience Research Reports*, 52: 75–83.
Vondrák D., Krause D., Hrubá J. & Kletetschka G., 2021: The paleolake Stifter Hollow and signs of the last stage of Quaternary glaciation in the Plešné Lake cirque. *Silva Gabreta*, 27: 1–15.

Received: 27 July 2022
Accepted: 2 January 2023